

## Knockout of Tmem70 alters biogenesis of ATP synthase and leads to embryonal lethality in mice

Marek Vrbacký<sup>1,†</sup>, Jana Kovalčíková<sup>1,8,†</sup>, Kallayanee Chawengsaksophak<sup>4,5</sup>, Inken M. Beck<sup>4</sup>, Tomáš Mráček<sup>1</sup>, Hana Nůsková<sup>1</sup>, David Sedmera<sup>2,7</sup>, František Papoušek<sup>3</sup>, František Kolář<sup>3</sup>, Margarita Sobol<sup>6</sup>, Pavel Hozák<sup>6</sup>, Radislav Sedlacek<sup>4,5</sup> and Josef Houštěk<sup>1,\*</sup>

<sup>1</sup>Department of Bioenergetics, <sup>2</sup>Department of Cardiovascular Morphogenesis, and <sup>3</sup>Department of Developmental Cardiology, Institute of Physiology of the Czech Academy of Sciences, <sup>4</sup>Czech Centre for Phenogenomics, <sup>5</sup>Laboratory of Transgenic Models of Diseases, Division BIOCEV, and <sup>6</sup>Laboratory of Biology of the Cell Nucleus, Institute of Molecular Genetics of the Czech Academy of Sciences, Prague, Czech Republic, <sup>7</sup>Institute of Anatomy, <sup>8</sup>First Faculty of Medicine, Charles University in Prague, Czech Republic.

† M.V. and J.K. contributed equally to this work

### \* To whom correspondence should be addressed:

Josef Houštěk, Institute of Physiology of the Czech Academy of Sciences, Vídeňská 1083, 14220 Prague 4, Czech Republic, Tel: +420 2 4106 2434, E-mail: [houstek@biomed.cas.cz](mailto:houstek@biomed.cas.cz)

## Abstract

TMEM70, a 21 kDa protein localized in the inner mitochondrial membrane, has been shown to facilitate the biogenesis of mammalian F<sub>1</sub>F<sub>0</sub> ATP synthase. Mutations of the *TMEM70* gene represent the most frequent cause of isolated ATP synthase deficiency resulting in a severe mitochondrial disease presenting as neonatal encephalo-cardiomyopathy (OMIM 604273). To better understand the biological role of this factor, we generated *Tmem70*-deficient mice and found that the homozygous *Tmem70*<sup>-/-</sup> knockouts exhibited profound growth retardation and embryonic lethality at approximately 9.5 days *post coitum*. Blue-Native electrophoresis demonstrated an isolated deficiency in fully assembled ATP synthase in the *Tmem70*<sup>-/-</sup> embryos (80% decrease) and a marked accumulation of F<sub>1</sub> complexes indicative of impairment in ATP synthase biogenesis that was stalled at the early stage, following the formation of F<sub>1</sub> oligomer. Consequently, a decrease in ADP-stimulated State 3 respiration, respiratory control ratio and ATP/ADP ratios, indicated compromised mitochondrial ATP production. *Tmem70*<sup>-/-</sup> embryos exhibited delayed development of the cardiovascular system and a disturbed heart mitochondrial ultrastructure, with concentric or irregular cristae structures. *Tmem70*<sup>+/-</sup> heterozygous mice were fully viable and displayed normal postnatal growth and development of the mitochondrial oxidative phosphorylation system. Nevertheless, they presented with mild deterioration of heart function. Our results demonstrated that *Tmem70* knockout in the mouse results in embryonic lethality due to the lack of ATP synthase and impairment of mitochondrial energy provision. This is analogous to *TMEM70* dysfunction in humans and verifies the crucial role of this factor in the biosynthesis and assembly of mammalian ATP synthase.

## Introduction

Mitochondrial ATP synthase ( $F_1F_0$ -ATP synthase, complex V), the key enzyme of cellular energy provision, produces ATP by utilizing the energy of a proton gradient across the mitochondrial membrane, generated by respiratory chain substrate oxidation. The ATP synthase complex is composed of 18 different subunits that form the globular, catalytic  $F_1$  part connected by two stalks with the proton-translocating membrane-spanning  $F_0$  part (1, 2). Two of the  $F_0$  subunits, a and A6L (ATP6 and ATP8) are encoded by the mitochondrial genome (3), while all the other ATP synthase subunits are nuclear encoded. In addition, at least three ancillary proteins, ATPAF1 (ATP11), ATPAF2 (ATP12) and TMEM70, are specifically involved in the biosynthesis and assembly of mammalian ATP synthase (4-8).

Inborn disorders of ATP synthase rank as some of the most severe metabolic diseases. They present as mitochondrial encephalo-cardio-myopathies and predominantly affect the pediatric population (9). Isolated ATP synthase defects can be caused by mutations in mtDNA (10) or in nuclear genes (11). Numerous mtDNA mutations in *MT-ATP6* coding for subunit a (12, 13) manifest mainly as neuropathy, ataxia and retinitis pigmentosa (NARP syndrome) or maternally inherited Leigh syndrome (MILS), while a rare mutation of *MT-ATP8* (A6L subunit of  $F_0$ ) presented as hypertrophic cardiomyopathy (14). A distinct group of isolated defects of ATP synthase (OMIM 604273) is represented by mutations in nuclear genes and, up to now, four of them have been identified as disease-causing (8, 15-17). Two of them, *ATP5A1* (16) and *ATP5E* (17) code for structural subunits  $\alpha$  and  $\epsilon$  of the  $F_1$  moiety of ATP synthase while the other two *ATP12* (*ATPAF2*) (15) and *TMEM70* (8) encode enzyme-specific ancillary biogenetic factors. All these defects share a similar biochemical phenotype of isolated enzyme deficiency – pronounced decrease in the content of assembled and functional ATP synthase complex (18). However, their incidences, mechanism of molecular

pathogenesis, clinical manifestation, and the course of disease progression, differ substantially. Mutations in either *ATP5A1*, *ATP5E* or *ATP12* are extremely rare in contrast to *TMEM70* which represents a mutational hotspot for ATP synthase deficiencies (7, 19). So far, about 20 different mutations of the human *TMEM70* gene were reported in more than 50 affected families (see (18, 20, 21)). Of these the homozygous c.317-2A>G mutation that removes the splicing site prior to the third exon of *TMEM70* is the most common (8). In fibroblasts derived from these patients, no TMEM70 protein can be detected, the content of fully assembled ATP synthase is severely reduced, and the amount of F<sub>1</sub> complexes is increased. This leads to diminished mitochondrial ATP production and elevated levels of mitochondrial membrane potential ( $\Delta\psi_m$ ) as ATP synthase capacity is insufficient to utilize the proton gradient generated by respiratory chain complexes. This phenotype can be completely rescued by complementation of affected fibroblasts with wildtype (wt) *TMEM70* (8).

TMEM70 is a 21 kDa protein containing two transmembrane regions, localized as a hair-pin in the inner mitochondrial membrane, and it is expressed at lower levels than structural subunits of ATP synthase (22, 23). Its regulatory role is directly linked to the biogenesis of ATP synthase, but its exact molecular function has not yet been described.

Animal models constitute a powerful tool for in the depth study of human mitochondrial pathologies *in vivo* and may ultimately help in elucidating the function of novel factors of mitochondrial biogenetic machinery. In the present study we describe a mouse model of TMEM70 deficiency, generated with the aim to verify and further characterize the role of TMEM70 protein at the organismal level. Knockout of the *Tmem70* gene in mouse caused embryonic lethality due to isolated deficiency of ATP synthase. This very well corresponded both structurally and functionally with the biochemical phenotype of inherited deficiency of TMEM70 factor in humans. This study represents the first direct

demonstration of the essential role of TMEM70 in the biogenesis and assembly of ATP synthase at levels necessary for mammalian embryonic development.

## Results

### ***Tmem70* homozygous knockout is embryonically lethal**

To characterize the biological role of TMEM70 *in vivo*, we produced a mouse with functional knockout of the *Tmem70* gene using publicly available embryonic stem cells *Tmem70*<sup>tm1a(KOMP)Wtsi</sup> (Fig. 1A).

Following germline transmission heterozygous *Tmem70*<sup>+/*flox*</sup> mice were interbred; however, no viable *Tmem70*-deficient mice (*Tmem70*<sup>*flox/flox*</sup> knockout) were born. The genotype correlated with the expression of *Tmem70* at the RNA level. The expression of *Tmem70* in E9.5 embryos in heterozygotes accounted for ~60% of that in wt mice, while *Tmem70* mRNA was undetectable in homozygous *Tmem70*<sup>*flox/flox*</sup> embryos (Fig. 1B). Genotyping of born animals revealed that other genotypes followed the expected Mendelian ratios (analyzed pups n = 212, *Tmem70*<sup>+/+</sup> n = 71, *Tmem70*<sup>+/*flox*</sup> n = 141). To find out how homozygotes die *in utero*, embryos from *Tmem70*<sup>+/*flox*</sup> mice intercrosses were dissected at embryonic days 8.5-9.5 *post coitum* and genotyped (Fig. 1C). Of 481 embryos analyzed, the following genotypes were detected: *Tmem70*<sup>*flox/flox*</sup> n = 100, *Tmem70*<sup>+/*flox*</sup> n = 260, *Tmem70*<sup>+/+</sup> n = 121 (the nulls and heterozygotes further denoted as *Tmem70*<sup>-/-</sup> and *Tmem70*<sup>+/-</sup>). All *Tmem70* null embryos exhibited a severe growth retardation phenotype (Fig. 1D).

### ***Tmem70*<sup>-/-</sup> embryos are severely deficient in mitochondrial ATP synthase**

As mutations of the human *TMEM70* gene cause isolated deficiency of ATP synthase, we investigated the biogenesis of ATP synthase in knockout embryos. We measured expression of the *Atp5A1* gene, coding for subunit  $\alpha$  of the ATP synthase catalytic moiety F<sub>1</sub>, but no difference between the *Tmem70* null and heterozygous or wt embryos (*Atp5A1/SDHA* mRNA in null was 96-100% of wt) was observed, pointing to a normal expression of ATP synthase

structural subunits. In contrast, the tissue content and composition of mitochondrial ATP synthase was strongly affected in knockout mouse embryos. Analysis by Blue-Native electrophoresis followed by Western blot immunodetection with an antibody against ATP synthase subunit F<sub>1</sub>- $\alpha$  showed an approx. 80 % decrease of the fully assembled ATP synthase complex (F<sub>1</sub>F<sub>0</sub>, CV) contrasting with a 3.5-4-fold accumulation of F<sub>1</sub>-complexes in homozygous *Tmem70*<sup>-/-</sup> knockout embryos (Fig. 2A), when compared with wt *Tmem70*<sup>+/+</sup> embryos. Heterozygous *Tmem70*<sup>+/-</sup> embryos did not differ from wt and contained normal amounts of ATP synthase complex, and only traces of free F<sub>1</sub> complex (Fig. 2B). This resulted in a 20-fold increase in the F<sub>1</sub>/F<sub>1</sub>F<sub>0</sub> ratio in *Tmem70*<sup>-/-</sup> embryos (Fig. 2C). A comparable decrease of the ATP synthase complex in the null embryos was observed with antibodies against structural subunits a and c of the membranous F<sub>0</sub> part of ATP synthase (F<sub>0</sub>-a and F<sub>0</sub>-c subunits). Importantly, this analysis further verified that accumulated subcomplex in *Tmem70*<sup>-/-</sup> embryos did not contain F<sub>0</sub> subunits and therefore represented a sole catalytic F<sub>1</sub> moiety of the enzyme. Hence, the alteration of ATP synthase biogenesis was stalled at an early stage, after the formation of F<sub>1</sub> catalytic head and it was not accompanied by accumulation of later assembly intermediates, such as F<sub>1</sub>-c complex. We also did not observe accumulation of any presumable F<sub>0</sub> intermediates or aggregates consisting of non-degraded F<sub>0</sub> subunits (Fig. 2A). ATPase in-gel activity staining further confirmed the diminished content of ATP synthase complex in *Tmem70*<sup>-/-</sup> null embryos (Fig. 2A) and showed that accumulated F<sub>1</sub> complexes retained ATPase hydrolytic activity.

Subsequent probing with antibodies against representative subunits of the respiratory chain complexes, succinate dehydrogenase - complex II (SDHA subunit), *bc*<sub>1</sub> complex - complex III (Core 1 subunit), and cytochrome *c* oxidase - complex IV (Cox4 subunit) showed near-normal content of respiratory chain enzymes in *Tmem70*<sup>-/-</sup> embryos compared with *Tmem70*<sup>+/+</sup> or *Tmem70*<sup>+/-</sup> embryos and demonstrated the isolated character of ATP synthase

deficiency (Fig. 2A). Overall, these biochemical studies clearly showed that knockout of the *Tmem70* gene selectively impairs ATP synthase biogenesis in mice.

### **Altered mitochondrial energetic function in *Tmem70*<sup>-/-</sup> embryos**

To test whether function of the mitochondrial oxidative phosphorylation system was affected by *Tmem70* knockout, we analyzed respiration in freshly prepared homogenates of E9.5 embryos with different substrates on a Seahorse XF<sup>e</sup> analyzer. *Tmem70*<sup>-/-</sup> embryos displayed much lower rates of ADP-stimulated (State 3) oxidation of respiratory chain substrates (pyruvate + glutamate + malate + succinate) normalized to respiratory chain content (SDHA content). The specific activity of oligomycin-sensitive oxidation of these substrates (State 3 - State 4) was decreased by 68-71 % in *Tmem70*<sup>-/-</sup> when compared to wt and heterozygous embryos (Fig. 3A), indicating an apparent decrease in mitochondrial ATP synthetic capacity in the null embryos. This translates into a two-fold decrease in the respiratory control ratio (State 3/State 4) in *Tmem70*<sup>-/-</sup> null embryos (Fig. 3A). When we analyzed the content of adenine nucleotides in E9.5 embryos by HPLC we have found that the ATP/ADP ratio in *Tmem70*<sup>-/-</sup> null embryos was also 2-fold decreased, indicating a depressed energetic state (Fig. 3B). Insufficient or altered function of ATP synthase can upregulate mitochondrial membrane potential and thus ROS production, due to increased electron leak from the mitochondrial respiratory chain (24-27). Immunodetection of antioxidant defense enzymes revealed upregulation in the content of mitochondrial Mn-dependent superoxide dismutase (SOD2) in *Tmem70*<sup>-/-</sup> null vs. heterozygous and wt embryos. The same tendency was observed for Cu/Zn-dependent SOD1, albeit here it did not reach statistical significance (Fig. 3C).

### **Developmental retardation of *Tmem70*<sup>-/-</sup> embryos**

Homozygous *Tmem70*<sup>-/-</sup> knockout embryos were considerably smaller at 9.5 days *post coitum* than their wild type littermates while the heterozygous embryos were unaffected (Fig. 1D). The average size of *Tmem70*<sup>-/-</sup> embryos was less than half of the controls, their body curvature was often still in a lordotic-like curvature, they had an open anterior neuropore (Fig. 1D, inset) and their somite number was <15 compared to the 25 somite stage of their wt and heterozygous littermates, all consistent with a one-day developmental delay (i.e. E8.5). Considering this developmental delay, the hearts reflected the retardation: they were significantly smaller, but showed normal looping (for achieved developmental stage) and were differentiated into proper compartments, i.e., atrium, ventricle with starting trabeculation, and the outflow tract (Fig. 1D and 4A). The colonization of cardiac cushions by mesenchymal cells was also considerably reduced, resembling the situation at E8.5 with only a few cells entering the cardiac jelly. Intravascular presence of erythrocytes indicated that functional circulation was already established. The hearts showed contractility at the time of embryo isolation, and the extent and intensity of smooth muscle  $\alpha$ -actin staining (marker or early myocardium) was normal.

Whole mount staining for the active form of caspase 3 showed only a few scattered cells in all genotypes. This indicates that widespread apoptosis is not a part of the mutant phenotype (not shown). Semithin sections (in addition to serial confocal sections) clearly demonstrated that the myocardium was on average composed from two cell layers (range 1-3). The connections between the cells appeared normal.

### **Mitochondrial ultrastructure is disturbed in *Tmem70*<sup>-/-</sup> knockout embryos**

ATP synthase has been recently implicated as an important structural factor of mitochondrial cristae formation (28-30). To further investigate the structural consequences of ATP synthase deficiency in *Tmem70*<sup>-/-</sup> mice we performed transmission electron microscopy (TEM) on

E9.5 embryos. TEM analysis detected pronounced changes in mitochondrial morphology in the heart as a result of *Tmem70*<sup>-/-</sup> knockout (Fig. 4B). Wild-type embryos contained  $1.3 \pm 0.1$  mitochondria per  $\mu\text{m}^2$  (n = 45 cells), with  $83.4 \pm 3.4$  % of mitochondria exhibiting normal ultrastructure. On the contrary, in *Tmem70*<sup>-/-</sup> mouse embryos  $80.5 \pm 1.3$  % of mitochondria displayed atypical shapes and fewer cristae with altered morphology (n = 45 cells; average density of mitochondria was  $1.4 \pm 0.3$  mitochondria per  $\mu\text{m}^2$ ). In particular, the classical arrangement of trabecular cristae was often replaced by concentric or irregular cristae structures.

### **Postnatal heart phenotype of *Tmem70*<sup>+/-</sup> heterozygous mice is affected**

*Tmem70*<sup>+/-</sup> heterozygous mice were analyzed at the age of 5 and 14 weeks and compared with wild type littermates, but no distinguishable differences were found in their growth parameters (body, heart weights). Blue-Native electrophoresis showed normal content of assembled ATP synthase without accumulation of F<sub>1</sub> intermediates, as well as normal content of respiratory chain complexes (Fig. S1). Detailed phenotypic characterization of mitochondrial energetic function showed unchanged parameters of substrate oxidation (State 3-ADP, State 3-FCCP, ATP production, sensitivity to oligomycin). Similarly, measurements of mitochondrial membrane potential did not reveal any changes in  $\Delta\psi_m$  at state 3 or state 4 (Fig. S2).

Despite the lack of a biochemical phenotype, we observed a mild systolic dysfunction of the heart left ventricle in *Tmem70*<sup>+/-</sup> mice by echocardiography. Decrease of the heart's left ventricle contractility represented by the parameter of fractional shortening was detected in *Tmem70*<sup>+/-</sup> mice compared to wt mice in both age groups (Table 1). In parallel, the systolic wall thickness which is related to a decreased fractional shortening, was significantly decreased at 14 weeks.



## Discussion

*TMEM70* was discovered as a disease-causing gene for neonatal encephalo-cardiomyopathy due to the isolated deficiency of ATP synthase in 2008 (8). Since then, numerous subsequent studies of affected families provided a compelling evidence that TMEM70 protein is essential for sustaining the physiological rates of ATP synthase biogenesis and thus for the full maintenance of mitochondrial energy provision by oxidative phosphorylation (for review see (18)). In parallel, biosynthesis, membrane assembly and native properties of TMEM70 protein have been characterized in detail (22, 23), but up to now, its exact role remains unclear. Unlike ATP11 or ATP12, the other two biogenetic factors of human ATP synthase, TMEM70 is specific for higher eukaryotes and cannot be studied in *Saccharomyces cerevisiae*, which lacks the ortholog of *TMEM70* gene (8). Animal models could therefore provide an important approach for further elucidation of TMEM70 function, analogous to numerous recent animal knockouts, which have significantly improved our knowledge of mitochondrial respiratory chain (RC) enzymes and their biogenetic factors (31, 32).

In our mouse model of *Tmem70* dysfunction, homozygous *Tmem70*<sup>-/-</sup> knockout resulted in a pronounced developmental delay and embryonic lethality at around the stage E9, demonstrating that *Tmem70* protein is required for early embryogenesis in mice. For the first time it showed the essential requirement of ATP synthase (and thus mitochondrial energy provision) for the early stages of mammalian prenatal development. Similar embryonic lethality was observed for homozygous knockouts of other respiratory chain structural components such as NDUFA5 (complex I subunit) (33), SDHD (complex II subunit) (34), RISP - Rieske iron sulfur protein (complex III subunit) (35) or their specific ancillary factors e.g. *Ndufs4* for complex I (36), *Cox15* for heme a biosynthesis (37) or *Cox17* and *Sco2* copper chaperones for complex IV (38, 39). While all these models convincingly

demonstrated requirement of active respiratory chain complexes for embryogenesis, knockout of yet another assembly factor for complex IV, Surf1 protein, had a very mild phenotype (40), contrasting with the mostly fatal SURF1 dysfunction in humans (41). This reflects potential tissue and species specific functions of some assembly factors, where mice can tolerate absence of Surf1, which is required for proper biogenesis of otherwise indispensable complex IV. Interestingly, in humans TMEM70 resembles SURF1 to some extent, as a small amount of the properly assembled ATP synthase is also formed even in the absence of TMEM70. However, ATP synthase levels were decreased by similar extent (60-70%) in all examined patient's tissues and cells (11, 42, 43), pointing to uniform necessity for TMEM70 function across all tissues. Mouse *Tmem70* knockout further indicates that the resulting ATP synthase deficiency may have a general character and can be even more severe in rodents.

The results of knockout of *Tmem70* in mouse support our hypothesis that TMEM70 is involved in the early stage of ATP synthase biogenesis (7). Analysis of *Tmem70*<sup>-/-</sup> embryos clearly showed that absence of Tmem70 factor prevents sufficient biosynthesis of functional ATP synthase, resulting in low content of complete ATP synthase complex and accumulation of assembly intermediate consisting of an F<sub>1</sub> catalytic moiety without any F<sub>0</sub> subunits (Fig. 3). This important observation indicated that the ATP synthase assembly process was stalled after F<sub>1</sub> oligomer formation, before it establishes contacts with the c-subunit ring, and thus prevented efficient formation of F<sub>1</sub>-rotor complex. These changes recapitulated observations regarding content and assembly forms of ATP synthase in human tissues and cells from affected individuals lacking TMEM70 (8, 11). Importantly, an identical phenotype could also be induced by *TMEM70* CRISPR-Cas9 knockout in HEK293 cells (Vrbacky et al., in preparation).

Analysis of ATP synthase in the *Tmem70* null embryos further confirmed that c-subunits, as well as other F<sub>0</sub> moiety subunits that are not incorporated into the holoenzyme,

are readily degraded. This removal of subunit c is in a sharp contrast with other types of ATP synthase deficiencies caused by mutation (17) or knockdown (44) of *ATP5E* gene encoding subunit  $\epsilon$ , or by knockdown of *ATP5C* and *ATP5D* genes for  $\gamma$  and  $\delta$  - the other two  $F_1$  central stalk subunits (45). In all these cases the ineffective formation of  $F_1$  is accompanied by the accumulation of strongly hydrophobic c subunits. Collectively, these data indicate that TMEM70 factor can be involved in establishing interactions of  $F_1$  with c subunit ring, and/or in regulation of the discharge of c subunits for proteolytic degradation. Mechanistically, TMEM70 could bind to  $F_1$  and stabilize it for formation of the complex with the c-oligomer (46), however, we were unable to detect direct interactions between TMEM70 and  $F_1$  or c subunits, despite extensive immunoprecipitation and crosslinking efforts (23). Theoretically, Tmem70 can also be involved in c-ring assembly. It has clearly been shown for bacterial c subunit, that it can undergo self-assembly into the c-oligomer without involvement of any other ATP synthase subunit and this was ascribed to the primary structure properties of the c subunit (47). However, it cannot be excluded, that the formation of c8 ring of higher eukaryotes may require an additional factor, which would be in line with Tmem70 evolutionary appearance (8). Further studies are needed to test other possibilities, such as involvement of additional adaptor protein(s) that would facilitate the regulatory role of TMEM70.

At the functional level, the *Tmem70* knockout altered energetic function of mitochondria in the null embryos. Respiratory measurements in wild type (+/+) and heterozygous (+/-) embryo homogenates showed tight coupling and well preserved intact mitochondria. As can be seen from oxygen consumption rates, the ATP synthase capacity became insufficient to fully utilize the  $H^+$  electrochemical gradient generated by the respiratory chain in -/- embryos. Consequently, the respiratory control ratio (RCR) and the ADP-stimulated respiration representing ATP synthesis, was strongly decreased. An

associated decrease in the ATP/ADP ratio showed that in addition the overall energetic state is compromised, apparently due to the impaired mitochondrial energy provision. Beside the low content of ATP synthase complex, accumulation of enzymatically active F<sub>1</sub> complexes unregulated by F<sub>0</sub> subunits may further exacerbate the overall energetic insufficiency as free F<sub>1</sub> driven hydrolysis of ATP in the mitochondrial matrix can further deplete the cellular ATP pool. While theoretically free F<sub>1</sub> could be inhibited by endogenous ATP synthase inhibitor IF<sub>1</sub>, its role *in vivo* seems to be more complex at high values of membrane potential (48) and may also include inhibition of the synthetic activity of ATP synthase (49). Such IF<sub>1</sub> action would further worsen the impact of ATP synthase deficiency.

Early embryonic development is associated with marked transitions in energy metabolism reflecting varying levels of oxygen *in utero* (50, 51). It changes from oxidative phosphorylation during early preimplantation stages to increasingly glycolytic throughout compaction and blastulation. Once chorioallantoic circulation is established and the heart begins to function, the embryo shifts back towards oxidative metabolism. Oxidative metabolism is inevitably connected with ROS formation, which in turn leads to the activation of antioxidant defense mechanisms (52). Analysis of *Tmem70*<sup>-/-</sup> embryos at E9 revealed upregulation of SOD1 and SOD2, indicative of higher levels of oxidative stress. This observation confirmed that the functional consequences of ATP synthase deficiency in mouse embryos include both the energy deprivation and the enhanced oxidative stress. This is reminiscent of the postnatal biochemical manifestation of human ATP synthase deficiency due to *TMEM70* mutations (26) and the same combination of decreased ATP production and enhanced ROS generation was also observed for mtDNA mutations in the ATP6 subunit (24). The two component pathology of ATP synthase deficiencies therefore seems to be a rather general phenomenon and explains why such deficiency is incompatible with normal embryonic development in mice.

In families affected by mutations in the *TMEM70* gene, frequent impairment of prenatal development was also reported, but it is much less severe than in mice (11, 19, 21, 43). Out of 25 cases with identical homozygous c.317-2A>G *TMEM70* mutation (preventing *TMEM70* protein synthesis), 68% of affected children were delivered prematurely and intrauterine growth retardation was present in 58% (birth weight 2040±471g, gestation age 36±2.6 weeks). Similarly, four of the six cases with other *TMEM70* mutations were born prematurely with birth weight below the 3rd percentile (53). Hence, the absence of *TMEM70* shows pronounced species-specific differences in embryonic lethality – with full penetrance in our C57BL/6n inbred mice but rather an occasional occurrence in humans, as only a few miscarriages have been reported in some of the affected families (11, 46, 54).

One of the clinical symptoms of human *TMEM70* mutations is early postnatal hypertrophic cardiomyopathy, reported in 76% of cases (19, 21). Prenatally, mild thickening of the cardiac chambers, and right sided clubfoot became evident at sonography at the 28<sup>th</sup> – 30<sup>th</sup> week of gestation (53). In our mouse knockout model the *Tmem70*<sup>-/-</sup> embryonic lethality corresponded to the stage when the heart becomes functionally essential for further development. However, despite developmental delay, no apparent structural changes and dysfunction could be found in hearts of null embryos. This indicates that the overall energetic insufficiency rather than heart malfunction itself was the critical determinant of embryonic survival. Most likely the embryos died before heart morphology could be affected.

While deficiency of *Tmem70* protein was lethal, postnatal development revealed haplosufficiency of *Tmem70* gene function in mice. *Tmem70*<sup>+/-</sup> heterozygous mice were viable and at the age of 4 months they did not show differences in growth parameters, function of mitochondrial oxidative phosphorylation system or structure and function of ATP synthase. Nevertheless, mild but significant deterioration of heart function was observed by echocardiography – this pinpoints the high energy demands of, and vulnerability of, the heart,

which is also the primary affected organ in TMEM70-lacking humans as well as in many other oxidative phosphorylation disorders (55).

In summary, we have generated a novel mouse model of genetic knockout of *Tmem70* gene that causes downregulation of ATP synthase biogenesis. It became stalled at the level of F<sub>1</sub> oligomer which led to critical impairment of mitochondrial energy provision, analogous to *TMEM70* dysfunction in humans. The resulting embryonic lethality and observed phenotypic changes convincingly demonstrated in the rodent model that TMEM70 ancillary factor is essential for maintaining biosynthesis and assembly of ATP synthase at the physiological rates necessary to cover the energetic demands of the developing mammalian organism.

## Materials and Methods

### Ethics Statement

Animal care and experiments were approved by the Animal Care Committees of the Institute of Physiology and Institute of Molecular Genetics of the Czech Academy of Sciences (study ID#174/2010) in compliance with national and institutional guidelines (ID#12135/2010-17210).

### Generation of *Tmem70*-deficient mice

*Tmem70*-deficient mice were generated using JM8.A4 embryonic stem (ES) cells harboring knockout first allele (*Tmem70*<sup>tm1a(KOMP)<sup>Wtsi</sup></sup>) obtained from the KOMP repository (trans-NIH Knock-Out Mouse Project, www.komp.org). Using laser-assisted technique ES cells were injected into 8-cell stage embryos of strain C57BL/6J-*Tyr*<sup>c-2J</sup> to generate chimeric mice. *Tmem70*tm1a<sup>+/-</sup> mice were crossed with Cre recombinase expressing strain (Gt(ROSA)26Sor<sup>tm1(ACTB-cre,-EGFP)<sup>Ics</sup>/Ics</sup>, (56)) to convert the tm1a allele into a tm1b allele.

Both *tm1a* and *tm1b* mice showed an identical phenotype - lethality at 9.5 dpc (E9.5) and thus *Tmem70tm1a* mice were used to analyze the lethal impact of *Tmem70* knockout and the ATP synthase biogenesis. Mice were provided food and water *ad libitum* and housed under 12 h light–dark cycle.

### **Collections and DNA analysis of mouse embryos**

Mouse embryos were harvested at several developmental stages from timed pregnant females. The morning of the vaginal plug was considered as embryonic day 0.5 (E0.5). Embryos were dissected out of the membranes under a dissection microscope and further processed as outlined below.

### **Genotyping**

Genotyping was performed on yolk sac or mouse tail lysates. Samples were incubated overnight at 56 °C in 30 µL (yolk sac) or 400 µL (tail) PCR buffer (10 mM Tris-HCl, 50 mM KCl, 2.5 mM MgCl<sub>2</sub>, 0.1 mg/mL Gelatin, 0.45% (v/v) IGEPAL, and 0.45% (v/v) Tween 20) containing Proteinase K (100 µg/mL). Lysates were diluted to 10 ng of DNA/µL with PCR grade water with following primer combinations: *Tm1a* - FW: TATATCCCCTCCCCGTTAG, REV: CACTGCAACTCGGCCTTTA, *Tm1b* - FW: ACGGTTTCCATATGGGGATT, REV: CACTGCAACTCGGCCTTTA, WT FW: GCATGCACCACCACTGTGTAG. *Tm1a* PCR products were cleaved by *Sac1* restriction enzyme for 3 h at 37 °C. *Tm1a* and *tm1b* PCR products were resolved by 1% agarose gel electrophoresis.

### **RT-PCR**

To perform quantitative RT-PCR whole embryo RNA was isolated using an RNase mini-kit (Qiagen) and cDNA was synthesized from 40 ng of RNA by reverse transcription (SCRIPT cDNA Synthesis Kit, Jena Biosciences). The following predesigned primer/probe sets (TaqMan Gene Expression Assays, Life Technologies) were used: *Tmem70* (Mm00466179\_m1), *Sdha* (Mm01352366\_m1), *Atp5a1* (Mm00431960\_m1), and *B2m* (Mm00437762\_m1). qPCR amplifications were carried out on a ViiA 7 instrument (Life Technologies) with the following cycling protocol: 95 °C for 15 min, and 40 cycles at 95 °C 20 s and 60 °C for 1 min. All reactions were done in duplicate and 1 µL of diluted (1:1) cDNA was used in each 10 µL reaction using HOT FIREPol probe qPCR Mix (Solis Biodyne).  $\Delta$ Ct was calculated for all genes. Standard curves for all genes were created by serially diluting wt embryo cDNA. The Ct of all genes was related to Ct of housekeeper reference *B2m*.

### **Electrophoresis and Western blot analysis**

Frozen embryos stored at -86 °C were pulverized in liquid nitrogen and homogenized with PBS with protease inhibitor cocktail (PIC, 1:500, Sigma P8340) in a glass-glass micro-homogenizer (1 mL, Fisher Scientific). Protein content was determined by a Bradford assay (BioRad). Tissue homogenates were solubilized for 20 min at 0 °C using 2 g n-dodecyl- $\beta$ -D-maltoside/g protein and centrifuged for 20 min at 30 000 g. Proteins in supernatants were analyzed by BN-PAGE, SDS-PAGE and 2D BN/SDS-PAGE followed by Western blot as described previously (22, 23). Gels were blotted onto PVDF membrane (Millipore) by semi-dry electrotransfer and immunodetected with primary antibodies to ATP synthase subunits F<sub>1</sub>- $\alpha$  (mouse polyclonal, clone 20D6 (57)), F<sub>0</sub>-a (rabbit polyclonal (58)), F<sub>0</sub>-c (rabbit polyclonal (57)), Complex II SDHA subunit (mouse monoclonal, Abcam ab14715), Complex III Core 1 subunit (mouse monoclonal, Abcam ab 110252) and Complex IV Cox4 subunit

(mouse monoclonal, Abcam ab14744). For a quantitative detection, the corresponding infrared fluorescent secondary antibodies (Alexa Fluor 680, Life Technologies; IRDye 800, Rockland Immunochemicals) were used. Fluorescence was detected using ODYSSEY infrared imaging system (LI-COR Biosciences) and the signal was quantified using Aida 3.21 Image Analyzer software (Raytest).

### **ATPase in-gel activity assay**

Enzyme in-gel activity staining was performed after separation of the respiratory complexes using BN-PAGE (BNE). The in-gel activity assay of the ATPase hydrolytic activity was performed as described (59).

### **Respiratory measurements**

Fresh mouse embryos were homogenized in Assay medium (70 mM sucrose, 220 mM mannitol, 10 mM  $\text{KH}_2\text{PO}_4$ , 5 mM  $\text{MgCl}_2$ , 2 mM HEPES, 1 mM EGTA, 0.2% BSA; pH 7.2) containing substrates for Complex I (10 mM pyruvate, 2 mM malate, 10 mM glutamate), 5  $\mu\text{M}$  cytochrome c, 2 mM ADP, and PIC (1:500, Sigma). Hand homogenization was performed in a glass-glass micro-homogenizer (1 mL, Fisher Scientific). Homogenates were transferred to XF-V7 24-well plates (Seahorse Bioscience) and spun down for 20 minutes at 2000 g, 4 °C to attach the homogenate to the plastic surface. Before measurement, the total volume in each well was adjusted to 500  $\mu\text{L}$  with Assay medium plus substrates (same as for homogenization). The oxygen consumption rate (OCR) was determined at 37 °C with complex I substrates/ADP and then after subsequent additions of 10 mM succinate, 2  $\mu\text{M}$  oligomycin, 4  $\mu\text{M}$  FCCP, and 0.4  $\mu\text{M}$  antimycin A. The data are presented as the OCR in picomoles  $\text{O}_2$  per minute. The respiratory control ratio (RCR) was calculated from the respiration values after adding succinate (State 3) and oligomycin (State 4).

### **Adenine nucleotide analysis**

Flash-frozen embryos stored in liquid nitrogen were homogenized and deproteinated by 6% (v/v) perchloric acid in a glass-glass micro-homogenizer, centrifuged, supernatant neutralized to pH = 7 by 0.4 M triethanolamine / 1.8 M KOH and the content of ATP and ADP was determined by HPLC as described in (60).

### **Whole mount confocal microscopy**

The embryos were isolated in ice-cold PBS, fixed overnight in 4% paraformaldehyde at 4 °C, then rinsed and stored in PBS at 4 °C. Prior to further processing, photographs of the embryos were taken on an Olympus SZX dissecting microscope. For whole mount immunohistochemistry (61), the embryos were permeabilized and blocked in normal goat serum with 0.1% Triton-X in TBS for 2 h, followed by 24 h incubation with the primary antibodies (alpha smooth muscle actin, clone 1A4, Sigma, 1:1,000, and the rat anti-mouse CD31 clone MEC13.3 from BD Pharmingen, 1:500). After 3x2 h rinsing with PBS, the samples were incubated for 24 h with the appropriate goat secondary antibodies (Jackson Immuno) coupled with Alexa488 (anti-rat) and rhodamine red (anti-mouse). Hoechst 33342 nuclear stain (1:100,000) was added to the secondary antibody solution. After thorough rinsing, the embryos were rapidly dehydrated in ethanol, cleared in xylene, and mounted into cavity slides (Fisher Scientific) in DEPEX permanent mounting media (Electron Microscopy Sciences) and coverslipped. After drying, the slides were examined on an upright Olympus FluoView confocal microscope using 4x-20x objective lenses. The images were assembled into plates and labeled using Adobe Photoshop. Digital image processing included background subtraction, level adjustment for each channel, and Unsharp Mask filtering.

### **Transmission Electron Microscopy**

Mouse embryos (E8.5, E9.5) were removed from mice, washed immediately in Sorensen's phosphate buffer (SB; 0.1 M, pH 7.2-7.4) at 37 °C and fixed with 2.5% glutaraldehyde in SB during 1-2 h at 4 °C (62). Then, fixed embryos were embedded into melted agarose at 37 °C, and agarose was allowed to harden on ice. Agarose-embedded embryos were post-fixed with 1% OsO<sub>4</sub> in SB, dehydrated in ethanol series, and embedded in Epon-Durkupan. Ultrathin sections (70-90 nm) were cut with Ultramicrotome Leica EM UC6, mounted on copper grids, contrasted with a saturated aqueous solution of uranyl acetate, and examined in FEI Morgagni 268 transmission electron microscope operated at 80 kV and in FEI TECNAI G2 20 LaB6 electron microscope operated at 200 kV (63). The images were captured using Mega View III CCD camera (Olympus Soft Imaging Solutions). Quantitative data are presented as mean ± standard deviation.

### **Echocardiography**

Transthoracic echocardiographic measurement of geometrical and functional parameters of the left heart ventricle (LV) was performed using GE Vivid 7 Dimension (GE Vingmed Ultrasound, Horten, Norway) with 12 MHz high resolution matrix probe M12-L. Animals were anesthetized by inhalation of 2% isoflurane (Forane, Abbott), placed on a heated table and their temperature (rectal thermometer RET-4, Physitemp Instruments) was maintained within 36.5 and 37.5 °C. For echocardiographic evaluation, the following diastolic and systolic dimensions were measured: cavity diameter (LVDd, LVDs), anterior wall thickness (AWTd, AWTs), posterior wall thickness (PWTd, PWTs) and heart rate (HR). The main functional parameter, fractional shortening (FS%) was derived from these dimensions by the following formula:  $FS\% = 100 \times (LVDd - LVDs) / LVDd$ . All dimensions were measured in

parasternal long and short axes view using two-dimensional and M-mode images. Repeated measurements in every view and mode were then averaged.

## **Acknowledgements**

This work was supported by Grant Agency of the Czech Republic (14-36804G), and Czech Academy of Sciences – CAS (RVO:67985823), Ministry of Education, Youth and Sports of the Czech Republic – MEYS CR (LL1204), and Grant agency for Medical Research (16-33018A). Purchase of the Seahorse instrument was supported by ERDF project Mitenal (CZ.2.16/3.1.00/21531).

JK was supported by Grant Agency of Charles University (726214), RS was supported by MEYS CR (LM2011032, LM2015040 and CZ.1.05/1.1.00/02.0109 - project BIOCEV) and CAS (RVO:68378050), MS and PH were supported by TACR (TE01020118), and MEYS CR (LM2015062 Czech-BioImaging).

ES cells used for this research project were generated by the trans-NIH Knock-Out Mouse Project (KOMP) and obtained from the KOMP Repository ([www.komp.org](http://www.komp.org)). We sincerely thank Ms. Alena Kvasilova (Institute of Anatomy, First Faculty of Medicine) for her expert help with whole mount immunostaining.

## **Conflict of Interest Statement**

None declared.

## References

- 1 Stock, D., Leslie, A.G. and Walker, J.E. (1999) Molecular architecture of the rotary motor in ATP synthase. *Science*, **286**, 1700-1705.
- 2 Walker, J.E., Collinson, I.R., Van Raaij, M.J. and Runswick, M.J. (1995) Structural analysis of ATP synthase from bovine heart mitochondria. *Methods Enzymol.*, **260**, 163-190.
- 3 Anderson, S., Bankier, A.T., Barrell, B.G., de Bruijn, M.H., Coulson, A.R., Drouin, J., Eperon, I.C., Nierlich, D.P., Roe, B.A., Sanger, F. *et al.* (1981) Sequence and organization of the human mitochondrial genome. *Nature*, **290**, 457-465.
- 4 Ackerman, S.H. and Tzagoloff, A. (2005) Function, structure, and biogenesis of mitochondrial ATP synthase. *Prog. Nucleic Acid Res. Mol. Biol.*, **80**, 95-133.
- 5 Zeng, X., Neupert, W. and Tzagoloff, A. (2007) The metalloprotease encoded by ATP23 has a dual function in processing and assembly of subunit 6 of mitochondrial ATPase. *Mol. Biol. Cell*, **18**, 617-626.
- 6 Osman, C., Wilmes, C., Tatsuta, T. and Langer, T. (2007) Prohibitins interact genetically with Atp23, a novel processing peptidase and chaperone for the F1Fo-ATP synthase. *Mol. Biol. Cell*, **18**, 627-635.
- 7 Houstek, J., Kmoch, S. and Zeman, J. (2009) TMEM70 protein - a novel ancillary factor of mammalian ATP synthase. *Biochim. Biophys. Acta*, **1787**, 529-532.
- 8 Cizkova, A., Stranecky, V., Mayr, J.A., Tesarova, M., Havlickova, V., Paul, J., Ivanek, R., Kuss, A.W., Hansikova, H., Kaplanova, V. *et al.* (2008) TMEM70 mutations cause isolated ATP synthase deficiency and neonatal mitochondrial encephalocardiomyopathy. *Nat. Genet.*, **40**, 1288-1290.
- 9 Houstek, J., Pickova, A., Vojtiskova, A., Mracek, T., Pecina, P. and Jesina, P. (2006) Mitochondrial diseases and genetic defects of ATP synthase. *Biochim. Biophys. Acta*, **1757**, 1400-1405.

- 10 Holt, I.J., Harding, A.E., Petty, R.K. and Morgan-Hughes, J.A. (1990) A new mitochondrial disease associated with mitochondrial DNA heteroplasmy. *Am. J. Hum. Genet.*, **46**, 428-433.
- 11 Houstek, J., Klement, P., Floryk, D., Antonicka, H., Hermanska, J., Kalous, M., Hansikova, H., Hout'kova, H., Chowdhury, S.K., Rosipal, T. *et al.* (1999) A novel deficiency of mitochondrial ATPase of nuclear origin. *Hum. Mol. Genet.*, **8**, 1967-1974.
- 12 Schon, E.A., Santra, S., Pallotti, F. and Girvin, M.E. (2001) Pathogenesis of primary defects in mitochondrial ATP synthesis. *Semin. Cell. Dev. Biol.*, **12**, 441-448.
- 13 DiMauro, S. and Schon, E.A. (2003) Mitochondrial respiratory-chain diseases. *N. Engl. J. Med.*, **348**, 2656-2668.
- 14 Jonckheere, A.I., Hogeveen, M., Nijtmans, L.G., van den Brand, M.A., Janssen, A.J., Diepstra, J.H., van den Brandt, F.C., van den Heuvel, L.P., Hol, F.A., Hofste, T.G. *et al.* (2008) A novel mitochondrial ATP8 gene mutation in a patient with apical hypertrophic cardiomyopathy and neuropathy. *J. Med. Genet.*, **45**, 129-133.
- 15 De Meirleir, L., Seneca, S., Lissens, W., De Clercq, I., Eyskens, F., Gerlo, E., Smet, J. and Van Coster, R. (2004) Respiratory chain complex V deficiency due to a mutation in the assembly gene ATP12. *J. Med. Genet.*, **41**, 120-124.
- 16 Jonckheere, A.I., Renkema, G.H., Bras, M., van den Heuvel, L.P., Hoischen, A., Gilissen, C., Nabuurs, S.B., Huynen, M.A., de Vries, M.C., Smeitink, J.A. *et al.* (2013) A complex V ATP5A1 defect causes fatal neonatal mitochondrial encephalopathy. *Brain*, **136**, 1544-1554.
- 17 Mayr, J.A., Havlickova, V., Zimmermann, F., Magler, I., Kaplanova, V., Jesina, P., Pecinova, A., Nuskova, H., Koch, J., Sperl, W. *et al.* (2010) Mitochondrial ATP synthase deficiency due to a mutation in the ATP5E gene for the F1 epsilon subunit. *Hum. Mol. Genet.*, **19**, 3430-3439.
- 18 Hejzlarova, K., Mracek, T., Vrbacky, M., Kaplanova, V., Karbanova, V., Nuskova, H., Pecina, P. and Houstek, J. (2014) Nuclear genetic defects of mitochondrial ATP synthase. *Physiol. Res.*, **63 Suppl 1**, S57-71.
- 19 Honzik, T., Tesarova, M., Mayr, J.A., Hansikova, H., Jesina, P., Bodamer, O., Koch, J., Magner, M., Freisinger, P., Huemer, M. *et al.* (2010) Mitochondrial encephalocardio-myopathy with early neonatal onset due to TMEM70 mutation. *Arch. Dis. Child.*, **95**, 296-301.

- 20 Diodato, D., Invernizzi, F., Lamantea, E., Fagiolari, G., Parini, R., Menni, F., Parenti, G., Bollani, L., Pasquini, E., Donati, M.A. *et al.* (2015) Common and Novel TMEM70 Mutations in a Cohort of Italian Patients with Mitochondrial Encephalocardiomyopathy. *JIMD Rep.*, **15**, 71-78.
- 21 Magner, M., Dvorakova, V., Tesarova, M., Mazurova, S., Hansikova, H., Zahorec, M., Brennerova, K., Bzduch, V., Spiegel, R., Horovitz, Y. *et al.* (2015) TMEM70 deficiency: long-term outcome of 48 patients. *J. Inherit. Metab. Dis.*, **38**, 417-426.
- 22 Hejzlarova, K., Tesarova, M., Vrbacka-Cizkova, A., Vrbacky, M., Hartmannova, H., Kaplanova, V., Noskova, L., Kratochvilova, H., Buzkova, J., Havlickova, V. *et al.* (2011) Expression and processing of the TMEM70 protein. *Biochim. Biophys. Acta*, **1807**, 144-149.
- 23 Kratochvilova, H., Hejzlarova, K., Vrbacky, M., Mracek, T., Karbanova, V., Tesarova, M., Gombitova, A., Cmarko, D., Wittig, I., Zeman, J. *et al.* (2014) Mitochondrial membrane assembly of TMEM70 protein. *Mitochondrion*, **15**, 1-9.
- 24 Mattiazzi, M., Vijayvergiya, C., Gajewski, C.D., DeVivo, D.C., Lenaz, G., Wiedmann, M. and Manfredi, G. (2004) The mtDNA T8993G (NARP) mutation results in an impairment of oxidative phosphorylation that can be improved by antioxidants. *Hum. Mol. Genet.*, **13**, 869-879.
- 25 Houstek, J., Mracek, T., Vojtiskova, A. and Zeman, J. (2004) Mitochondrial diseases and ATPase defects of nuclear origin. *Biochim. Biophys. Acta*, **1658**, 115-121.
- 26 Mracek, T., Pecina, P., Vojtiskova, A., Kalous, M., Sebesta, O. and Houstek, J. (2006) Two components in pathogenic mechanism of mitochondrial ATPase deficiency: energy deprivation and ROS production. *Exp. Gerontol.*, **41**, 683-687.
- 27 Baracca, A., Sgarbi, G., Mattiazzi, M., Casalena, G., Pagnotta, E., Valentino, M.L., Moggio, M., Lenaz, G., Carelli, V. and Solaini, G. (2007) Biochemical phenotypes associated with the mitochondrial ATP6 gene mutations at nt8993. *Biochim. Biophys. Acta*, **1767**, 913-919.
- 28 Dudkina, N.V., Sunderhaus, S., Braun, H.P. and Boekema, E.J. (2006) Characterization of dimeric ATP synthase and cristae membrane ultrastructure from *Saccharomyces* and *Polytomella* mitochondria. *FEBS Lett.*, **580**, 3427-3432.

- 29 Strauss, M., Hofhaus, G., Schroder, R.R. and Kuhlbrandt, W. (2008) Dimer ribbons of ATP synthase shape the inner mitochondrial membrane. *EMBO J.*, **27**, 1154-1160.
- 30 Davies, K.M., Strauss, M., Daum, B., Kief, J.H., Osiewacz, H.D., Rycovska, A., Zickermann, V. and Kuhlbrandt, W. (2011) Macromolecular organization of ATP synthase and complex I in whole mitochondria. *Proc. Natl. Acad. Sci. U S A*, **108**, 14121-14126.
- 31 Torraco, A., Peralta, S., Iommarini, L. and Diaz, F. (2015) Mitochondrial Diseases Part I: mouse models of OXPHOS deficiencies caused by defects in respiratory complex subunits or assembly factors. *Mitochondrion*, **21**, 76-91.
- 32 Iommarini, L., Peralta, S., Torraco, A. and Diaz, F. (2015) Mitochondrial Diseases Part II: Mouse models of OXPHOS deficiencies caused by defects in regulatory factors and other components required for mitochondrial function. *Mitochondrion*, **22**, 96-118.
- 33 Peralta, S., Torraco, A., Wenz, T., Garcia, S., Diaz, F. and Moraes, C.T. (2014) Partial complex I deficiency due to the CNS conditional ablation of Ndufa5 results in a mild chronic encephalopathy but no increase in oxidative damage. *Hum. Mol. Genet.*, **23**, 1399-1412.
- 34 Piruat, J.I., Pintado, C.O., Ortega-Saenz, P., Roche, M. and Lopez-Barneo, J. (2004) The mitochondrial SDHD gene is required for early embryogenesis, and its partial deficiency results in persistent carotid body glomus cell activation with full responsiveness to hypoxia. *Mol. Cell. Biol.*, **24**, 10933-10940.
- 35 Hughes, B.G. and Hekimi, S. (2011) A mild impairment of mitochondrial electron transport has sex-specific effects on lifespan and aging in mice. *PLoS One*, **6**, e26116.
- 36 Ingraham, C.A., Burwell, L.S., Skalska, J., Brookes, P.S., Howell, R.L., Sheu, S.S. and Pinkert, C.A. (2009) NDUFS4: creation of a mouse model mimicking a Complex I disorder. *Mitochondrion*, **9**, 204-210.
- 37 Viscomi, C., Bottani, E., Civiletto, G., Cerutti, R., Moggio, M., Fagiolari, G., Schon, E.A., Lamperti, C. and Zeviani, M. (2011) In vivo correction of COX deficiency by activation of the AMPK/PGC-1alpha axis. *Cell. Metab.*, **14**, 80-90.
- 38 Takahashi, Y., Kako, K., Kashiwabara, S., Takehara, A., Inada, Y., Arai, H., Nakada, K., Kodama, H., Hayashi, J., Baba, T. *et al.* (2002) Mammalian copper chaperone Cox17p has an

- essential role in activation of cytochrome C oxidase and embryonic development. *Mol. Cell. Biol.*, **22**, 7614-7621.
- 39 Yang, H., Brosel, S., Acin-Perez, R., Slavkovich, V., Nishino, I., Khan, R., Goldberg, I.J., Graziano, J., Manfredi, G. and Schon, E.A. (2010) Analysis of mouse models of cytochrome c oxidase deficiency owing to mutations in Sco2. *Hum. Mol. Genet.*, **19**, 170-180.
- 40 Dell'agnello, C., Leo, S., Agostino, A., Szabadkai, G., Tiveron, C., Zulian, A., Prella, A., Roubertoux, P., Rizzuto, R. and Zeviani, M. (2007) Increased longevity and refractoriness to Ca(2+)-dependent neurodegeneration in Surf1 knockout mice. *Hum. Mol. Genet.*, **16**, 431-444.
- 41 Shoubridge, E.A. (2001) Nuclear genetic defects of oxidative phosphorylation. *Hum. Mol. Genet.*, **10**, 2277-2284.
- 42 Havlickova Karbanova, V., Cizkova Vrbacka, A., Hejzlarova, K., Nuskova, H., Stranecky, V., Potocka, A., Kmoch, S. and Houstek, J. (2012) Compensatory upregulation of respiratory chain complexes III and IV in isolated deficiency of ATP synthase due to TMEM70 mutation. *Biochim. Biophys. Acta*, **1817**, 1037-1043.
- 43 Sperl, W., Jesina, P., Zeman, J., Mayr, J.A., Demeirleir, L., VanCoster, R., Pickova, A., Hansikova, H., Houst'kova, H., Krejcik, Z. *et al.* (2006) Deficiency of mitochondrial ATP synthase of nuclear genetic origin. *Neuromuscul. Disord.*, **16**, 821-829.
- 44 Havlickova, V., Kaplanova, V., Nuskova, H., Drahota, Z. and Houstek, J. (2010) Knockdown of F1 epsilon subunit decreases mitochondrial content of ATP synthase and leads to accumulation of subunit c. *Biochim. Biophys. Acta*, **1797**, 1124-1129.
- 45 Pecina, P., Nůsková, H., Havlíčková, V., Houšťek, J. (2012) The role of mitochondrial ATP synthase central stalk subunits g and d in the activity and assembly of the mammalian enzyme. *Biochim. Biophys. Acta*, **1817**, S20-S21.
- 46 Torraco, A., Verrigni, D., Rizza, T., Meschini, M.C., Vazquez-Memije, M.E., Martinelli, D., Bianchi, M., Piemonte, F., Dionisi-Vici, C., Santorelli, F.M. *et al.* (2012) TMEM70: a mutational hot spot in nuclear ATP synthase deficiency with a pivotal role in complex V biogenesis. *Neurogenetics*, **13**, 375-386.

- 47 Arechaga, I., Butler, P.J. and Walker, J.E. (2002) Self-assembly of ATP synthase subunit c rings. *FEBS Lett.*, **515**, 189-193.
- 48 Lippe, G., Sorgato, M.C. and Harris, D.A. (1988) Kinetics of the release of the mitochondrial inhibitor protein. Correlation with synthesis and hydrolysis of ATP. *Biochim. Biophys. Acta*, **933**, 1-11.
- 49 Formentini, L., Pereira, M.P., Sanchez-Cenizo, L., Santacatterina, F., Lucas, J.J., Navarro, C., Martinez-Serrano, A. and Cuezva, J.M. (2014) In vivo inhibition of the mitochondrial H<sup>+</sup>-ATP synthase in neurons promotes metabolic preconditioning. *EMBO J.*, **33**, 762-778.
- 50 Harvey, A.J., Kind, K.L. and Thompson, J.G. (2002) REDOX regulation of early embryo development. *Reproduction*, **123**, 479-486.
- 51 Clough, J.R. (1985) Energy metabolism during mammalian embryogenesis. *Biochem. Soc. Trans.*, **13**, 77-79.
- 52 Ufer, C. and Wang, C.C. (2011) The Roles of Glutathione Peroxidases during Embryo Development. *Front. Mol. Neurosci.*, **4**, 12.
- 53 Spiegel, R., Khayat, M., Shalev, S.A., Horovitz, Y., Mandel, H., Hershkovitz, E., Barghuti, F., Shaag, A., Saada, A., Korman, S.H. *et al.* (2011) TMEM70 mutations are a common cause of nuclear encoded ATP synthase assembly defect: further delineation of a new syndrome. *J. Med. Genet.*, **48**, 177-182.
- 54 Braczynski, A.K., Vlaho, S., Muller, K., Wittig, I., Blank, A.E., Tews, D.S., Drott, U., Kleinle, S., Abicht, A., Horvath, R. *et al.* (2015) ATP synthase deficiency due to TMEM70 mutation leads to ultrastructural mitochondrial degeneration and is amenable to treatment. *Biomed. Res. Int.*, **2015**, 462592.
- 55 Brunel-Guitton, C., Levtova, A. and Sarsman, F. (2015) Mitochondrial Diseases and Cardiomyopathies. *Can. J. Cardiol.*, **31**, 1360-1376.
- 56 Birling, M.C., Dierich, A., Jacquot, S., Herault, Y. and Pavlovic, G. (2012) Highly-efficient, fluorescent, locus directed cre and FlpO deleter mice on a pure C57BL/6N genetic background. *Genesis*, **50**, 482-489.

- 57 Jesina, P., Tesarova, M., Fornuskova, D., Vojtiskova, A., Pecina, P., Kaplanova, V., Hansikova, H., Zeman, J. and Houstek, J. (2004) Diminished synthesis of subunit a (ATP6) and altered function of ATP synthase and cytochrome c oxidase due to the mtDNA 2 bp microdeletion of TA at positions 9205 and 9206. *Biochem. J.*, **383**, 561-571.
- 58 Dubot, A., Godinot, C., Dumur, V., Sablonniere, B., Stojkovic, T., Cuisset, J.M., Vojtiskova, A., Pecina, P., Jesina, P. and Houstek, J. (2004) GUG is an efficient initiation codon to translate the human mitochondrial ATP6 gene. *Biochem. Biophys. Res. Commun.*, **313**, 687-693.
- 59 Wittig, I., Karas, M. and Schagger, H. (2007) High resolution clear native electrophoresis for in-gel functional assays and fluorescence studies of membrane protein complexes. *Mol. Cell. Proteomics*, **6**, 1215-1225.
- 60 Flachs, P., Novotny, J., Baumruk, F., Bardova, K., Bourova, L., Miksik, I., Sponarova, J., Svoboda, P. and Kopecky, J. (2002) Impaired noradrenaline-induced lipolysis in white fat of aP2-Ucp1 transgenic mice is associated with changes in G-protein levels. *Biochem. J.*, **364**, 369-376.
- 61 Miller, C.E., Thompson, R.P., Bigelow, M.R., Gittinger, G., Trusk, T.C. and Sedmera, D. (2005) Confocal imaging of the embryonic heart: how deep? *Microsc. Microanal.*, **11**, 216-223.
- 62 Soplop, N.H., Patel, R. and Kramer, S.G. (2009) Preparation of embryos for electron microscopy of the Drosophila embryonic heart tube. *J. Vis. Exp.*, in press.
- 63 Tan, A.S., Baty, J.W., Dong, L.F., Bezawork-Geleta, A., Endaya, B., Goodwin, J., Bajzikova, M., Kovarova, J., Peterka, M., Yan, B. *et al.* (2015) Mitochondrial genome acquisition restores respiratory function and tumorigenic potential of cancer cells without mitochondrial DNA. *Cell. Metab.*, **21**, 81-94.

## Legends to figures

**Figure 1.** *Tmem70* knockout mouse. **(A)** Scheme of the knockout first allele (tm1a) with inserted neomycin cassette and production of tm1b knockout without neomycin cassette. **(B)** RT-PCR quantification of *Tmem70* mRNA (normalized to the expression of housekeeping *B2m* mRNA) confirms the lack of *Tmem70* transcript, n=2. **(C)** Genotyping of E9.5 embryos by restriction analysis of *Tmem70* PCR products (+/+ allele has 1125 bp and -/- allele has 777 bp) confirms the knockout. **(D)** Optical microscopy of wildtype (+/+), heterozygous (+/-), and retarded null (-/-) E9.5 embryos. OT – heart outer tract, V – ventricle, A – atrium, arrow points to open neuroporus anterior, scale bar 1 mm.

**Figure 2.** ATP synthase deficiency in *Tmem70*<sup>-/-</sup> embryos. **(A)** BN-PAGE separation of ATP synthase and respiratory chain complexes using dodecylmaltoside-solubilized proteins (2 g/g protein) of wt (+/+) null (-/-) and heterozygous (+/-) *Tmem70* knockout E9 embryos, ATPase in gel activity and WB detection with antibodies to ATP synthase (subunits F<sub>1</sub>-α, F<sub>0</sub>-c, F<sub>0</sub>-a), Complex II (CII, SDHA subunit), Complex III (CIII, Core 1 subunit), Complex IV (CIV, Cox4 subunit). **(B)** WB quantification of ATP synthase content with respect to CII (F<sub>1</sub>F<sub>0</sub> – complex of ~ 600 kDa, F<sub>1</sub> – subassembly of ATP synthase catalytic part of ~ 370 kDa). **(C)** Relative content of F<sub>1</sub> and F<sub>0</sub>F<sub>1</sub>, n = 2–3. Data are mean±SD, \* p≤0.05, \*\* p≤0.01, \*\*\* p≤0.001.

**Figure 3.** Altered mitochondrial energetic function in *Tmem70*<sup>-/-</sup> embryos. **(A)** Seahorse oxygraphy of the whole embryo homogenates with respiratory substrates pyruvate + malate + succinate. ADP-stimulated, oligomycin-sensitive respiratory rates (normalized to CII content) and respiratory control ratio RCR<sub>ADP</sub> were expressed in % of wt embryos values. **(B)**

ATP/ADP nucleotide content ratio in whole embryo extracts. **(C)** The level of superoxide dismutases in whole embryo extracts. SOD1 and SOD2 content was detected by SDS-PAGE and WB and normalized to CII content. Data are mean $\pm$ SD,  $n \geq 6$  in **A**, 5 in **B**, 6 in **C**, wt (+/+), null (-/-) and heterozygous (+/-) E9.5 embryos were used. \*  $p \leq 0.05$ , \*\*  $p \leq 0.01$ , \*\*\*  $p \leq 0.001$

**Figure 4.** Impaired morphology of *Tmem70*<sup>-/-</sup> embryos **(A)** Whole mount immunohistochemistry; confocal microscopy of retarded heart of null (-/-) embryo in comparison with wt (+/+) and heterozygous (+/-) E9.5 embryos: OT – outer tract, LV – left ventricle, LA – left atrium, NA – neuroporus anterior; SMA (alpha smooth muscle actin), red – myocardium; CD31, green – endocardium; Hoechst 33342, blue – nuclei; arrows point to emerging ventricular trabeculation, scale bar 100  $\mu$ m. **(B)** Electron microscopy of disturbed cristae morphology of null (-/-) compared to wt (+/+) heart mitochondria of E9.5 embryos. M – mitochondria, MF – myofibrils, LM – lysed mitochondria, N – nucleus, scale bar 1  $\mu$ m.

## Tables

**Table 1.** Weight parameters and impaired systolic function of the left ventricle (LV) detected by echocardiography in 5- and 14-week-old *Tmem70*<sup>+/-</sup> mice compared to *Tmem70*<sup>+/+</sup> mice.

AWTd – diastolic anterior wall thickness, LVDd – diastolic cavity diameter, PWTd – diastolic posterior wall thickness, AWTs – systolic anterior wall thickness, LVDs – systolic cavity diameter, PWTs – systolic posterior wall thickness, FS – fractional shortening, HR - heart rate, (BW) - body weight and (HW) - heart weight. Data are mean±SD values from 5-weeks-old mice (n=9) and 14-weeks-old mice (n=10-11); \* p<0.05, \*\* p<0.01, \*\*\* p<0.001.

|                     | 5 weeks                      |                              | 14 weeks                     |                              |
|---------------------|------------------------------|------------------------------|------------------------------|------------------------------|
|                     | <i>Tmem70</i> <sup>+/+</sup> | <i>Tmem70</i> <sup>+/-</sup> | <i>Tmem70</i> <sup>+/+</sup> | <i>Tmem70</i> <sup>+/-</sup> |
| <b>AWTd (mm)</b>    | 0.62 ± 0.03                  | 0.63 ± 0.04                  | 0.70 ± 0.07                  | 0.63 ± 0.05 *                |
| <b>LVDd (mm)</b>    | 3.71 ± 0.22                  | 3.60 ± 0.16                  | 4.30 ± 0.40                  | 4.10 ± 0.34                  |
| <b>PWTd (mm)</b>    | 0.62 ± 0.06                  | 0.64 ± 0.05                  | 0.69 ± 0.07                  | 0.62 ± 0.03 *                |
| <b>AWTs (mm)</b>    | 1.02 ± 0.08                  | 0.98 ± 0.08                  | 1.12 ± 0.09                  | 0.94 ± 0.09 ***              |
| <b>LVDs (mm)</b>    | 2.24 ± 0.17                  | 2.33 ± 0.12                  | 2.78 ± 0.32                  | 2.89 ± 0.37                  |
| <b>PWTs (mm)</b>    | 1.06 ± 0.08                  | 1.04 ± 0.1                   | 1.13 ± 0.09                  | 0.98 ± 0.1 **                |
| <b>FS (%)</b>       | 39.41 ± 2.15                 | 35.4 ± 2.41 **               | 35.5 ± 2.68                  | 29.9 ± 4.26 **               |
| <b>HR</b>           | 504 ± 46                     | 521 ± 53                     | 472 ± 36                     | 501 ± 43                     |
| <b>BW (g)</b>       | 18.72 ± 1.61                 | 18.85±0.87                   | 28.56±2.17                   | 28.42±1.75                   |
| <b>HW (mg)</b>      | 91±6.75                      | 91±4.81                      | 130±18.1                     | 124±9.6                      |
| <b>HW/BW (mg/g)</b> | 4.9±0.35                     | 4.8±0.2                      | 4.5±0.4                      | 4.4±0.3                      |

## Abbreviations

F<sub>1</sub>, catalytic part of ATP synthase; F<sub>o</sub>, membrane-embedded part of ATP synthase; WB, western blot

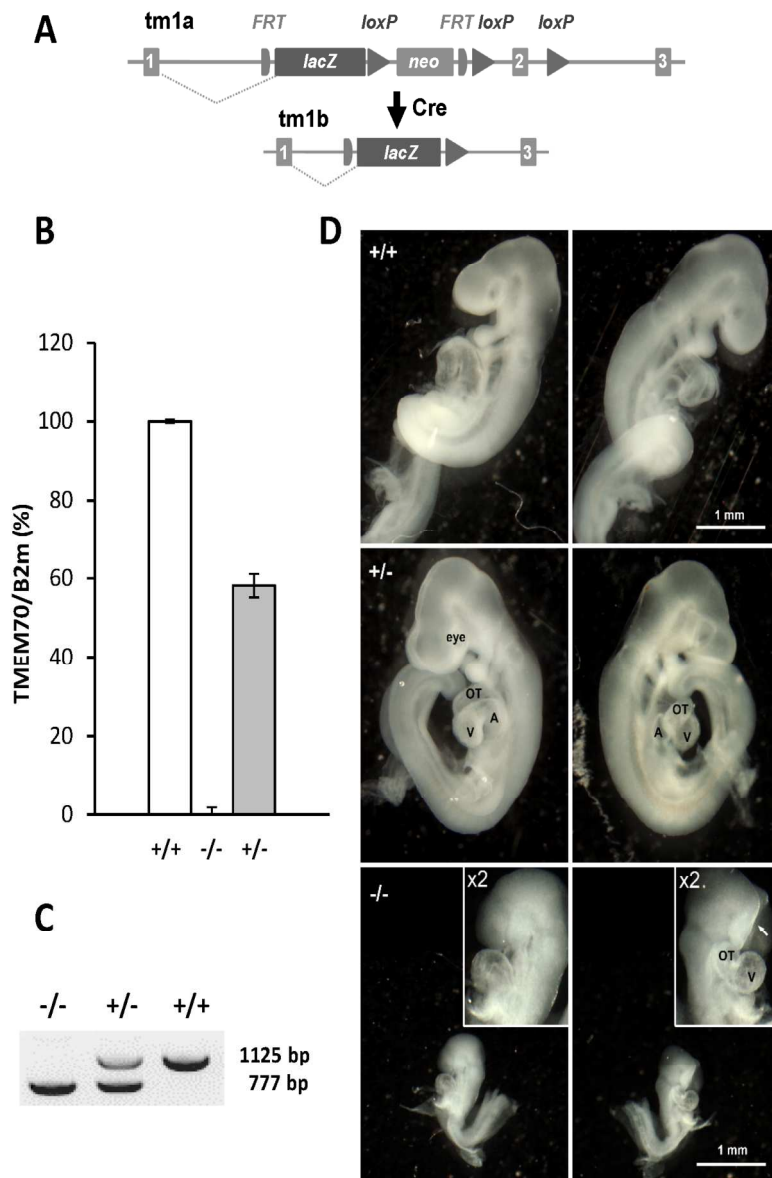


Fig. 1

176x266mm (300 x 300 DPI)

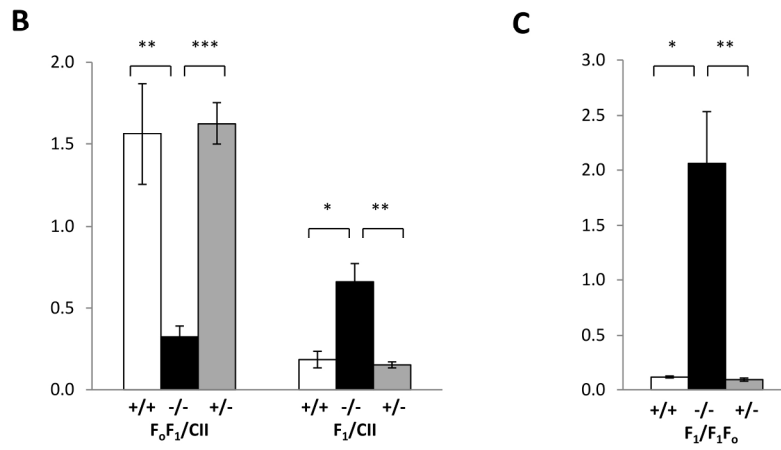
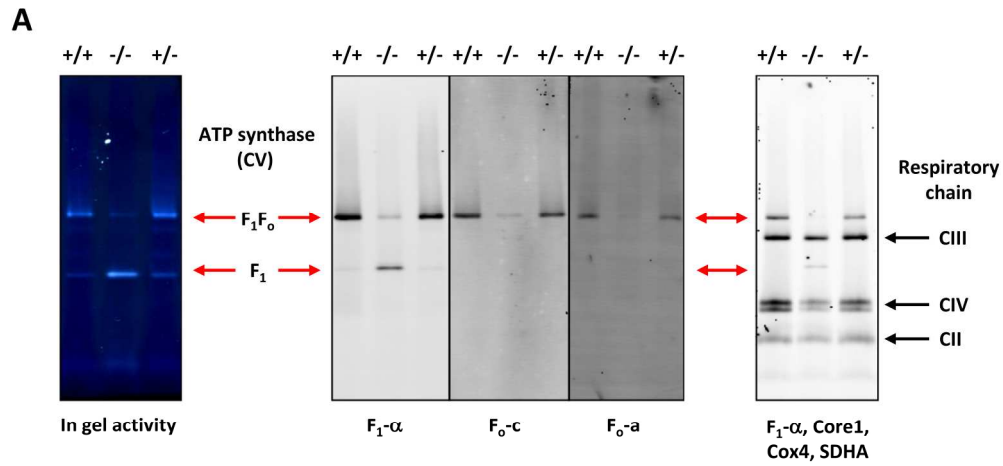


Fig. 2

216x204mm (300 x 300 DPI)

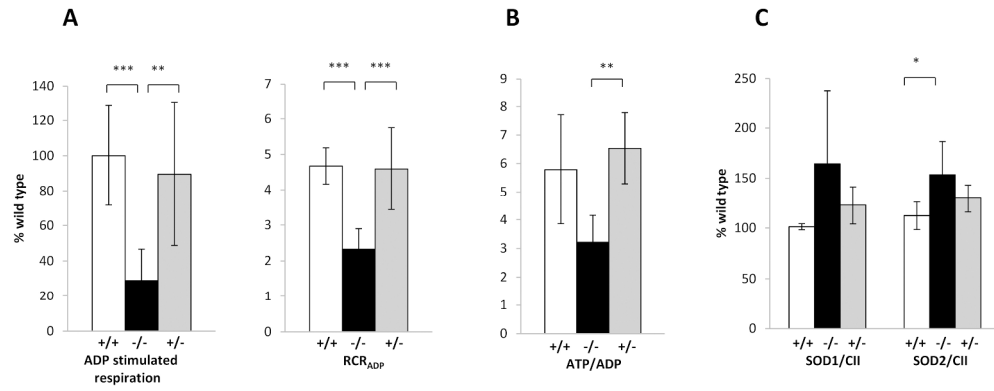


Fig. 3

283x110mm (300 x 300 DPI)

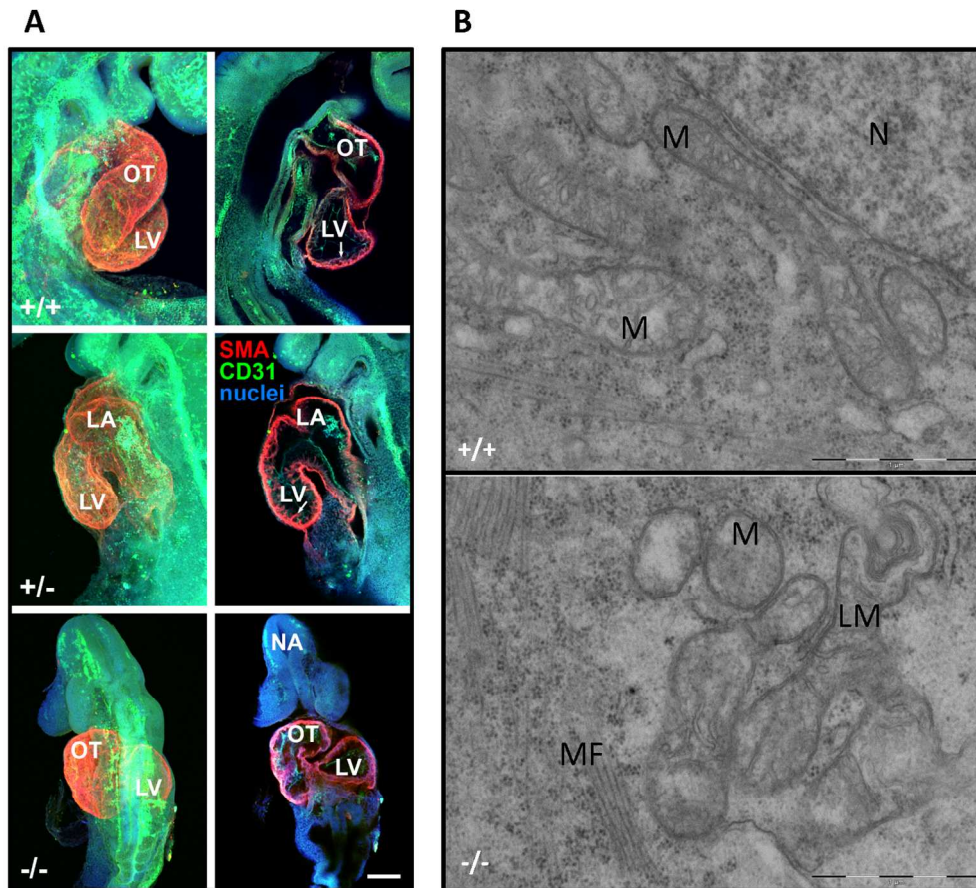


Fig. 4

181x162mm (220 x 220 DPI)